Advanced Materials Research *Online: 2011-07-04*
ISSN: 1662-8985, Vol. 278, pp 265-270
doi:10.4028/www.scientific.net/AMR.278.265

Microstructure and Mechanical Properties of an Advanced Nickel-Based Superalloy in the as-HIP Form

J.R. May[1,a], M.C. Hardy[2,b], M.R.Bache[1,c], D.D. Kaylor[3,d]
[1]Materials Research Centre, School of Engineering, Swansea University, Singleton Park, Swansea, SA2 8PP, UK
[2]Rolls-Royce plc, PO Box 31, Moor Lane, Derby DE24 8BJ, UK
[3]ATI Powder Metals, 1001 Robb Hill Road, Oakdale, Pennsylvania, 15071, USA
[a]196735@swansea.ac.uk, [b]m.c.hardy@rolls-royce.com, [c]m.r.bache@swansea.ac.uk, [d]david.kaylor@atipowder.com

Key words: RR1000, superalloy, powder metallurgy, hot isostatic pressing, heat treatment

Abstract. This study evaluates the suitability of as-hot isostatically pressed (HIP) RR1000 for non-critical applications in aero-engine components. RR1000, an advanced powder nickel-based superalloy, was developed for disc rotor components in aero-engines. For these critical applications, the consolidated alloy powder particles are extruded to break down carbide and oxide networks, known as prior particle boundaries (PPBs), and to refine the structure into a fine grain size for isothermal forging. In this study, hot isostatically pressed compacts, made from two different powder particle size fractions have been assessed following heat treatments below and above the gamma prime solvus temperature. A microstructural evaluation shows a greater degree of PPB decoration occurs in the finer powder particle size fraction. Following a super-solvus heat treatment these PPBs pin grain boundaries of the fine powder particle size compacts, whilst the reduction of PPB decoration in coarse powder particle compacts allows significant grain growth. Tensile test results of as-HIP RR1000 show, good yield strengths, ultimate tensile strengths and ductility, which are comparable with extruded and isothermal forged RR1000 disc material. Dwell crack propagation tests show that finer powder particle size compacts, which have received a sub-solvus heat treatment, give the highest crack growth rates; whilst the remaining material conditions show markedly improved crack growth resistance. In conclusion, as-HIP RR1000 demonstrates clear potential for use in non-critical applications, employing either powder particle size fraction used in this study subject to the appropriate solution heat treatment.

Introduction

RR1000 is a third generation γ' strengthened gas turbine nickel disc alloy, [1,2] designed to achieve the high levels of creep resistance and damage tolerance at the elevated temperatures required for modern civil jet engine discs. The complex chemistry of RR1000, requires that the alloy be manufactured by powder metallurgy to avoid macro segregation, which can occur in billet manufactured via cast and wrought processes. However, it is well reported [3-6] that superalloys produced via a powder metallurgy production route can suffer from PPB precipitate networks. In addition, inclusions can be introduced from the contact of the molten alloy with refractories such as those found in the vacuum induction melting (VIM) furnace, tundish and nozzle. For critical rotating components, PPB networks can be broken up through thermo-mechanical processing steps such as extrusion and forging operations, while large inclusions can be removed through sieving of the raw powder, before can filling, typically to sub-53 μm for RR1000 when used in disc material. The requirement to sieve powder for critical components creates surplus 'oversize' powder, which can be used in subsequent VIM heats.

However, using powder metal alloys in the HIP form can provide cost reductions for superalloy components presently manufactured from the more traditional cast and wrought techniques. This is due to the fewer processing steps required for as-HIP manufacture and reductions in material input from use of net or near net shape manufacture. This study evaluates the suitability of using as-HIP RR1000 for non-critical aerospace components, which may reduce component cost, and increase powder yields in manufacture.

Material Manufacture

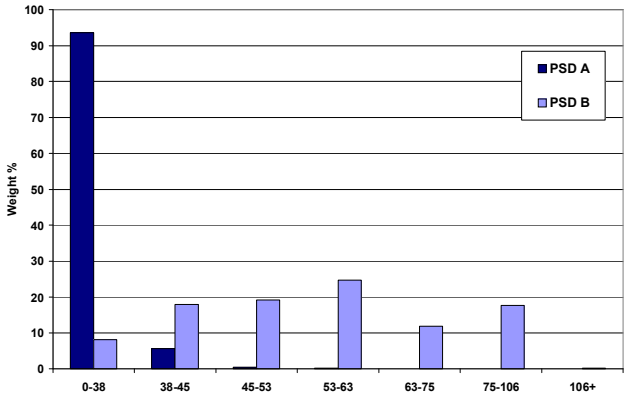

Figure 1. RR1000 powder particle distributions.

For this study two HIP compacts measuring approximately 15 cm in length and 7 cm in diameter were supplied by ATI Powder Metals in mild steel HIP containers. The powder was manufactured via melting in a VIM crucible followed by argon gas atomisation (AGA).

The powder used in this study was a blend of several heats and sieved to two different powder size distributions (PSD) shown in Fig. 1. One of the containers was filled with PSD A, whilst the second was filled with the coarser PSD B. Once filled, the containers were out gassed, sealed, and then HIP'd. The compositions of the two compacts met the required composition specification for RR1000 [2]. The oxygen and nitrogen levels for compact PSD A were 0.0172 and 0.0038 weight percent respectively. The oxygen and nitrogen levels for the coarser powder PSD B compact where 0.0139 and 0.0027 weight percent respectively.

The two compacts were sectioned into two halves, with either a sub- or supersolvus heat treatment given to each half, creating four different material conditions. The subsolvus heat treatment consisted of a 1130°C 2 hour solution treatment and the supersolvus heat treatment a 1170°C 2 hour solution treatment. Following a bench air cool, the compacts received an age treatment of 760°C for 16 hours. Thermocouple data from a compact heat treated at 1170°C showed a cooling rate of approximately 1.2˚C/s. The cooling rate influences γ' precipitate size and shape, in addition to grain boundary (GB) morphology and therefore determines the mechanical properties [7].

Microstructure and Grain Size

Microstructures for all material conditions were examined (Fig. 2) and the grain size measured by the mean linear intercept method. The average grain size for PSD A and PSD B compacts given a subsolvus heat treatment is 5 and 6 μm respectively. Heat treatment above the γ' solvus gives marked differences in the microstructure and grain size depending on the starting powder size distribution. The compact produced from PSD A given a supersolvus heat treatment shows an average grain size of 10 μm, whilst the compact produced from PSD B gives an average grain size of 21 μm for the same heat treatment. All microstructures from both sub- and supersolvus heat treatments show some GBs that are relatively spherical, implying Zener pinning of the GBs by the PPBs, [3,6]. This is most apparent in the PSD A compact material.

The PPBs found in as-HIP superalloys can occur from oxygen pick up and the segregation of elements to the powder particle surfaces [3-5]. During HIPing further carbides can precipitate at prior particle surfaces, and oxides can act as nuclei for their formation [5]. It follows that, PPBs are commonly made up of oxides, carbides and oxy-carbides. These can often consist of the heavier alloying elements such as Hf oxides, and Ta MC type carbides, in addition to lighter elements such as Ti. The heavy elemental constituents in the PPB precipitates make them prominent under SEM backscattered electron imaging mode. Typical examples of the PPB networks are shown in Fig. 3, showing PSD A and PSD B compact microstructures after a supersolvus heat treatment. From these

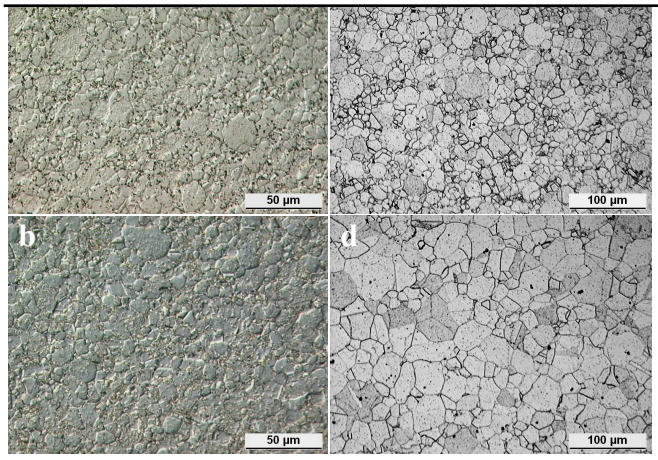

Figure 2. Optical microscopy images of as-HIP RR1000 showing similarity of microstructures between PSD A (a) and PSD B (b) compact material after exposure to a subsolvus heat treatment. Remaining images show differences between PSD A (c) and PSD B (d) compact material after exposure to super solvus heat treatment.

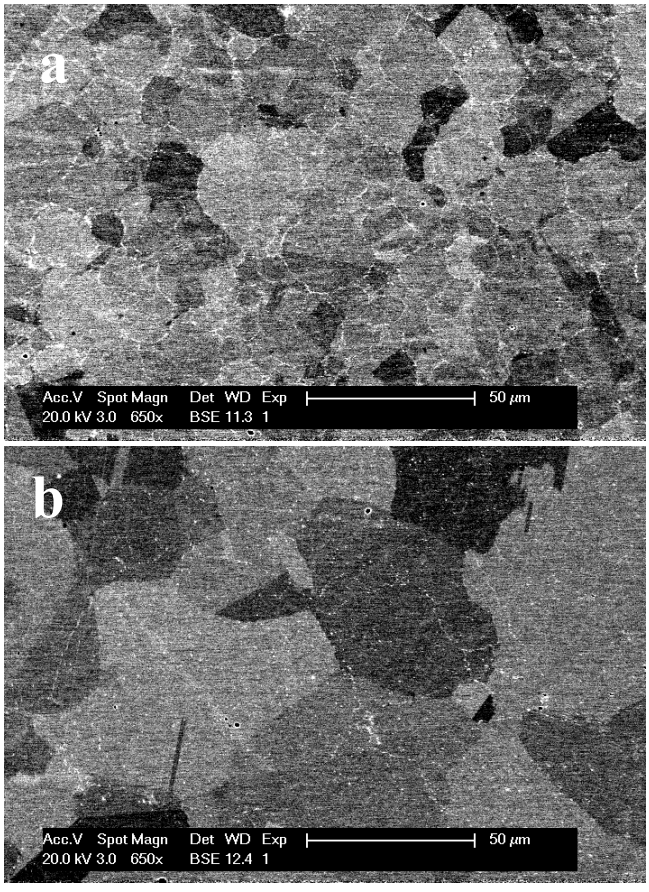

Figure 3. SEM backscattered electron images of PPB precipitates in as-HIP RR1000 following supersolvus heat treatment, viewed in the as polished condition. (a) shows PSD A as HIP material, (b) shows PSD B as HIP material.

images it appears that the coarser powder PSD B compact material shows a less continuous PPB network, with greater distance between individual precipitates.

The finer powder used in the PSD A compact material shows an increase in oxygen content compared with PSD B compact material, which is thought to be due to a greater surface area available for the pick up of oxygen on powder particle surfaces [4]. The increase and more continuous nature of the PPB precipitates in PSD A material, as seen in Fig. 3, is surmised to cause a greater degree of GB pinning. Therefore a smaller grain size is produced in PSD A compact material compared to the coarser powder PSD B compact given the same supersolvus heat treatment. In compacts solution heat treated at subsolvus temperatures this marked difference in grain size and morphology is not seen. This is because the GBs are pinned by coarse γ' precipitates formed during the slow cool from the HIP temperature during consolidation.

Mechanical Properties

Tensile Properties. Tensile testing was performed at room temperature and 700°C with two tests being conducted for each material condition and test temperature. A strain rate of $5x10^{-5}s^{-1}$ was used below the yield point and $1.3x10^{-3}s^{-1}$ above. Fig. 4 shows the average tensile strengths, which compare well with extruded and isothermally forged RR1000 disc material at all test temperatures. Good ductility values (~20%) were also obtained for all material conditions and test temperatures. The reduction in yield strength of the coarse powdered supersolvus condition is consistent with the Hall-Petch relationship [8].

The room temperature fracture surfaces for tensile specimens from PSD A and PSD B powder compacts, having received a supersolvus heat treatment, are shown in Fig. 5. Both PSD A and PSD B powder compacts show frequent 'socket and ball' features which are common in as-HIP superalloy tensile fracture surfaces [3,4]. These features form where failure occurs along prior particles boundaries. It was evident that ductile voids on the surface of socket and ball features have been nucleated by the oxide and carbide PPB precipitates. It is

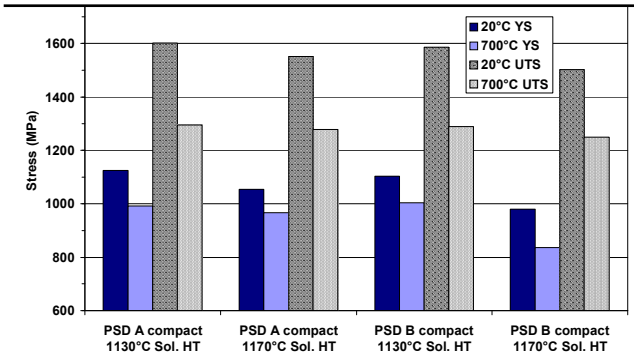

Figure 4. Yield strength and ultimate tensile strength of as-HIP RR1000 at room temperature and 700°C for the different powder fractions and solution heat treatments.

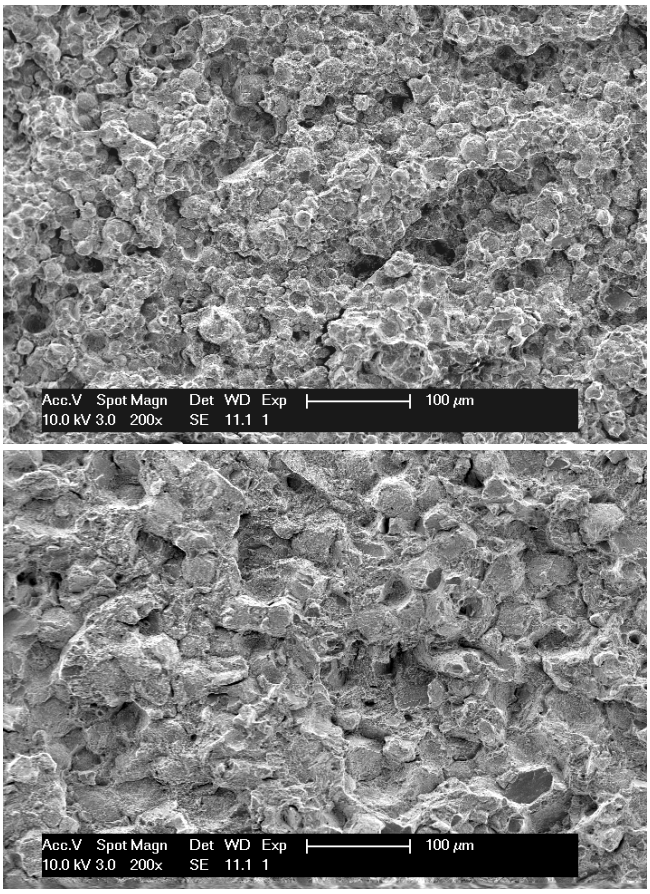

Figure 5. Secondary electron SEM images of fracture surfaces from room temperture tensile tests of as-HIP RR1000. Images (a) and (b) are supersolvus heat treated material from PSD A and PSD B compact material respectively.

proposed that the coalescence of these voids during tensile straining has caused the fracture along the PPBs.

The fracture surface appearance of PSD A and PSD B compact material differ when given a supersolvus heat treatment. The finer powder PSD A compact material shows fracture surfaces similar to the subsolvus material, whilst the coarser powdered PSD B compact material often has more faceted features, which become more prominent at the higher test temperatures. This is attributed to shear between ductile failure points.

Socket and ball features appear to be more numerous in the PSD A compacts. While the PSD B compact tensile fracture surfaces are characterised by less numerous, but larger socket and ball features. It is probable that the reduction in PPB decoration for the coarse powder compacts has reduced pinning of GBs at PPB locations; therefore the frequency of GB and PPB intersection is reduced. As a consequence, the intergranular failure is less often characterised by a socket and ball feature.

Dwell Crack Growth. Dwell fatigue crack growth testing was performed using a 1-120-1-1 trapezoidal cycle on corner crack test pieces. Dwell was applied at peak load with an R ratio of 0.1, with all testing carried out at 700°C. Fig. 6 details the results and shows the effect of different powder size fractions and heat treatments on dwell crack growth rates.

The effect of heat treatment and grain size on dwell crack growth follows expectation. The larger grain size material obtained from PSD B compact with the supersolvus heat treatment shows a reduction in the rate of dwell crack growth when compared with the fine grain subsolvus heat treated PSD B material. This is consistent with work conducted on fine and coarse grained RR1000 disc material [2]. It is well documented that stress assisted oxygen diffusion at elevated temperatures plays a crucial role in embrittlement of GBs and increasing crack propagation rates at elevated temperatures in polycrystalline superalloys [9,10]. A smaller grain size gives an increased GB density ahead of the crack tip, giving a smaller diffusion path and increasing the rate of oxygen diffusion down the GBs.

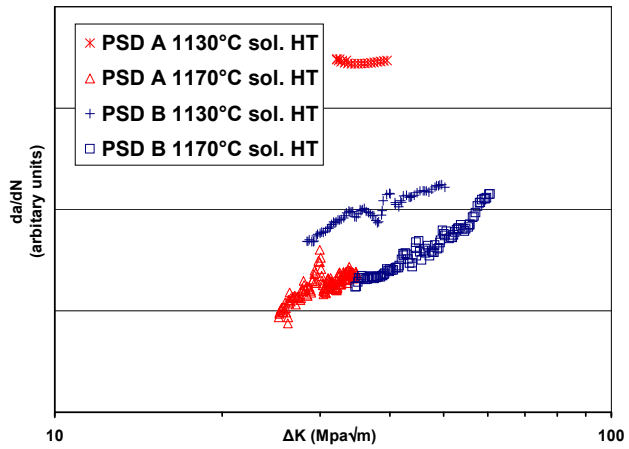

Figure 6. Relative crack growth rates for different powder size fractions and solution heat treatments tested at 700°C for as-HIP RR1000.

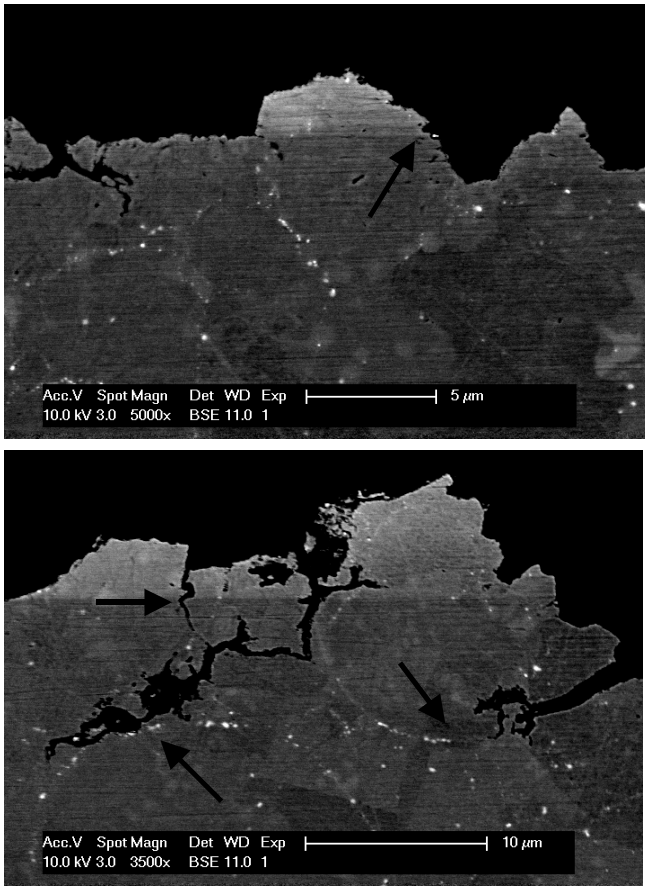

Figure 7. Dwell crack path in profile for as-HIP RR1000 PSD A material having received a subsolvus solution heat treatment. (a) ΔK = 34 MPa√m, crack path following PPB precipitates, (b) ΔK = 40 MPa√m, secondary cracking along PPB regions. Crack growth direction in each example is right to left.

The PSD A compact material shows a much greater variation in dwell crack growth rates depending on the heat treatment received. Surprisingly, PSD A compact material having received a supersolvus heat treatment shows equivalency to PSD B compact material that received the same supersolvus heat treatment despite the differences in grain size between PSD A and PSD B compacts of 10 μm and 21 μm respectively.

However the subsolvus heat treated PSD A material shows a far greater increase in crack growth rate than the other material conditions. Fig. 7 shows a metallographic section, prepared orthogonal to the main plane of fracture at the top of the image, to demonstrate the interaction between the crack and the local microstructure. It is clear that the crack tip frequently followed PPBs for this material condition, which was less so for the other material conditions.

The following factors may explain why PSD A compact material receiving a subsolvus heat treatment has a significantly higher crack propagation rate than the other material conditions. The fine grain size would be expected to increase the amount of stress assisted oxygen diffusion due to a reduced diffusion path distance, as previously mentioned. However, the subsolvus heat treatment also does not cause significant GB migration; consequently many of the GBs delineate PPB precipitates. The associated increase in carbides and oxides along the GBs will hinder GB sliding and slip mechanisms. Consequently, since the GBs cannot accommodate strains from these high temperature deformation mechanisms, they fracture. Furthermore, the density of these PPBs and GBs ahead of the crack tip is higher for the PSD A compact material than for the PSD B compact material receiving the same subsolvus heat treatment, explaining the higher rate for the PSD A subsolvus heat treated material.

The reduction in crack growth rate for PSD A compact material receiving a supersolvus heat treatment is thought to be due to grain growth and the associated GB migration. As explained earlier, the larger grain size reduces dwell crack growth rates, however the GB migration will also reduce the occurrence of GB and PPB intersection, reducing crack growth rate.

Summary and Conclusions

The microstructure, tensile and crack propagation properties of RR1000 have been evaluated in the as-HIP form for sub- and supersolvus heat treatment conditions, using two different powder fractions. Both powder fractions show PPB decoration. However, PPB density is greater in the finer powder compact material (PSD A) due to the higher surface area of the powder, resulting in higher bulk oxygen content, and an increase in PPB density. The results show that as-HIP RR1000 is characterised by a fine grain size (~6 μm) for both PSD A and PSD B powder compacts when given a subsolvus heat treatment. A supersolvus heat treatment produces a finer grain size in PSD A compact material of 10 μm due to pinning from PPB network while grains grow to 21 μm in PSD B compact material due to a reduced PPB density.

It has been shown that good ductility is obtained in all material conditions at both room temperature and 700°C, moreover yield and ultimate tensile strengths are comparable with extruded and isothermally forged RR1000. Crack growth properties for PSD B compact material are considered good. Compact material from PSD A shows equivalent crack growth rates when given a supersolvus heat treatment, but performs less well when a subsolvus heat treatment is applied. The reduced performance is considered to be caused by the combination of increased PPB density, small grain size and intersection of the GB and PPBs.

This preliminary study of the microstructure and properties of as-HIP RR1000 demonstrates that this alloy variant has the potential to be used in non-critical applications, from either a fine or coarse powder particle size fraction used in this study when given the appropriate solution heat treatment.

Acknowledgements

Rolls-Royce plc and the UK Engineering and Physical Sciences Research Council (EPSRC) are acknowledged for their financial support. ATI Powder Metals is acknowledged for provision of materials and contribution to the publication. Finally, the financial support from the Armourers and Brasiers' Livery Company to enable presentation of this work is gratefully acknowledged.

References

[1] M.C. Hardy, B. Zirbel, G. Shen, R. Shankar: TMS Superalloys (2004), p. 83-90.

[2] R.J. Mitchell, J.A. Lemsky, R. Ramanathan, H.Y. Li, K.M. Perkins, L.D. Connor: TMS Superalloys (2008), p. 347-356.

[3] R. Thamburaj, A.K. Koul, W. Wallace, M.C. de Malherbe: Modern Developments in Powder Metallurgy, Vol.16, (1985), p. 635-673.

[4] G. Appa Rao, M. Srinivas, D.S. Sarma: Mater. Sci. & Eng. A, (2006), p. 84-99.

[5] C. Marquz, G. L'Esperance, A.K. Koul: The International Journal of Powder Metallurgy, Vol.25, No.4, (1989), p. 301-308.

[6] M. Oktay Alniak, F. Bedir: Mater. Sci. & Eng. B, Vol. 130, (2006), p. 254-263.

[7] R. J. Mitchell, M.C. Hardy, M. Preuss, S. Tin: TMS superalloys (2004), p.361-370.

[8] W. D. Callister, Jr, in: *Fundamentals of Materials Science and Engineering*, John Wiley & Sons, Inc. (2005) second edition.

[9] S. Everitt, M.J. Starnik, P.A.S. Reed: TMS superalloys (2008), p. 741-750.

[10] R. Molins, G. Hochstetter, J.C. Chassaigne, E. Andrieu: Acta. Mater. Vol. 45, No.2, (1997), p. 663-674.